

Ocean Reverberation Suppression via Matrix Completion with Sensor Failure

Li-ya XU¹, Bin LIAO¹, Hao ZHANG², Peng XIAO¹, Jian-jun HUANG¹

¹ College of Electronics and Information Engineering, Shenzhen University,
Shenzhen 518060, China

² School of Marine Science and Technology, Northwestern Polytechnical University,
Xian 710072, China

Corresponding author: Peng XIAO, llyswan@hotmail.com

Abstract

As one of the most important physical phenomena of underwater acoustics, ocean reverberation is a common and strong interference which significantly degrades the performance of target bearing estimation. Meanwhile, sensor failure is inevitable in actual sonar deployment as the underwater scene is complicated. Therefore, it is a challenge for acoustic localization in the ocean reverberation with sensor failure. To address this issue, we propose an improved approach based on the principle of low rank characteristics of matrix in this paper. Firstly, we utilize Hankel structured matrix to counteract the problem of sensor failure. Then, the algorithm of matrix completion (MC) based on ℓ_1 -norm and ℓ_2 -norm are exploited to recover the true signal matrix from the corrupted received matrix. Numerical results demonstrate that compared with other related methods, the ℓ_1 -norm provides better capability in the probability of recovery and shows the best robustness of bearing estimation with the narrow beam width and low sidelobe. Moreover, the proposed approach verifies the performances of reverberation suppression and achieves high resolution of localization.

Keywords: direction of arrival (DOA), MC, low rank, ocean reverberation, sensor failure.

I Introduction

There exist various irregular scatterers in the ocean, such as marine lives, sediment particles, air bubbles, water masses, as well as roughness of sea surface and seafloor. The inhomogeneity generated by all these random scatterers forms a scattering field [1]. Similar to the long, slow and quivering sounds, ocean reverberation caused by scattering is one of the most important physical phenomena of underwater acoustics. According to the scattering sources, ocean reverberation can be divided into three categories, i.e., volume reverberation, sea surface reverberation, and seafloor reverberation [2]. Besides the ambient noise, ship noise, and so on, reverberation is known to be a common and strong interference in source localization. It is generated along with the transmit signal, and hence is closely related to the transmit signal itself. Additionally, it is also related to the propagation characteristics of sound field. Usually, the target signal is overwhelmed by reverberation, which severely limits the effective working distance and degrades the performance of sonar system. Fig. 1 shows the the acoustic localization with a vertical line

array (VLA) in ocean reverberation environment. As reverberation is formed by the superposition of a large number of random scatterers at the received sonar, it is a random process. In general, it is challenging to suppress reverberation under ocean reverberation background.

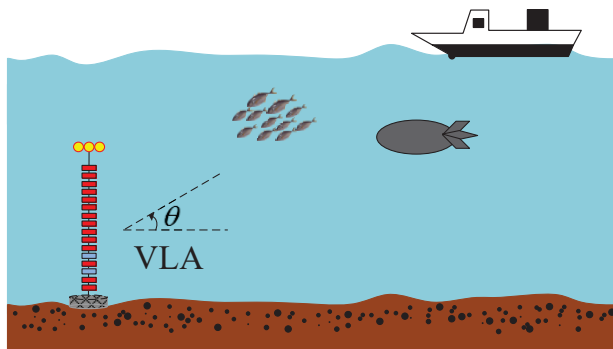


Fig. 1: DOA estimation with a VLA in ocean reverberation environment.

Many works have investigated reverberation suppression to improve the constant false alarm probability, especially for weak targets in the ocean. When combining the reverberation with transmit signals, the transmit waveform can be designed to reduce the influence of reverberation on the target, but it still needs to be analyzed by signal processing algorithms to extract the actual waveforms information [3, 4]. At the receiver, the reception directivity can be improved by increasing the azimuth direction aperture for reverberation suppression [5, 6]. According to the theory of normal mode, the acoustic signals can be composed of different modes. The reverberation usually has a high-order mode, and the filtering of normal mode can improve the signal-to-reverberation ratio (SRR), where a group or a low-order mode is chosen to enhance the target signal. The disadvantage of this method is that the choice of the normal mode heavily depends on the ocean environment and source depth [7, 8]. Besides, the background of reverberation can be normalized by adaptive beamforming algorithm [5, 9, 10]. However, it requires efficient estimation of the correlation matrix, and the estimation error will increase because of the instability. In addition, the classic matched processing method can be performed to use the transmit signal as a reference for coherent compression. Nevertheless, this method only performs well in white noise background. Therefore, a generalized matched filtering method [11] is firstly modified to whiten the reverberation by using the parametric model filtering with a recursive procedure. Meanwhile, the copy of sound field and the optimum focusing filtering are mainly used to reduce the mismatch error. Furthermore, the concept of time-reversal in acoustics is also derived from the method of phase conjugate in the frequency domain in optics. [12] used the time-reversal process to focus the acoustic energy on the target position, thereby effectively enhancing

the target echo to improve the SRR. [13, 14] proposed a time-reversal processing based on reverberation groove method and carried out an experimental demonstration. However, the zero point of reverberation in the specified distance and the excitation of the time-reversal array are not set. Due to the sparse property in detection circumstances, compressed sensing (CS) is utilized for target estimation [15]. It is demonstrated that the results of estimation achieved by CS beamforming have a higher azimuth resolution and higher detection ability than the conventional beamforming methods [16–18]. The detection of sparse target can be implemented in fractional Fourier transform, which exhibits an improved localization performance [19, 20]. Moreover, based on the difference between the reverberation and target signal, the method of principal component analysis (PCA) is used to suppress the reverberation. It does not require prior statistical knowledge and deterministic models, and hence it is highly adaptable [21, 22].

DOA estimation is one of the main approaches for acoustic localization. Note that the array processing algorithms in the ocean are generally based on the assumption of absence of errors in the hydrophone. Undesirably, in practical applications, due to the effects of hydrophone technologies, deployment methods, device aging and ocean environment, corrupted hydrophones with sensor failure are inevitable. Fig. 1 shows two corrupted hydrophones (marked with blue) in the VLA. The corrupted hydrophones will destroy the geometric distribution structure of the array. For example, a corrupted element will make the uniform line array lose the geometric symmetry, thereby reducing the array gain. The most direct method is to replace the corrupted hydrophones. However, it is difficult to implement when the sonar array has been placed in water because the acoustic data cannot be easily obtained in the experiment. Accordingly, reconstruction algorithms of the acoustic data can be used to reduce the influence of the corrupted sonar array and avoid the human and material resources incurred by replacing the hydrophones. Moreover, if the probability of corrupted array is taken into account in the early stage of data processing, the effect on array signal processing can be prevented.

For the corrupted array, there are the weight re-optimization of the remaining normal array elements and the reconstruction of contaminated array signals. According to the desired array pattern, the weight of the remaining normal array elements can be re-optimized, so that the directional pattern formed by the effective elements is as close as possible to the original one. The sidelobe level caused by the corrupted array elements can be suppressed by conjugate gradient method [23], quadratic constrained linear optimization [24], maintaining fixed nulls [25], adaptive weight reconstruction [26], and orthogonal methods [27]. To overcome the limitations on a long distance and huge computing quantity, these methods of weight

re-optimization are not easy to achieve as all the weights must be readjusted. The basic idea of signal reconstruction is to use the received data of the normal array elements to reconstruct the data of the corrupted array elements by interpolation or optimization algorithms. For a uniform linear array, the signal received by adjacent array elements has only a fixed phase difference, so the output of corrupted array elements can shift the phase according to the normal array element output. This method is relatively simple for single source but complicated for multiple sources. Generally, adjacent [28] or all [29] normal array elements can be used to reconstruct the output signal. Besides bilinear programming [30], cumulants [31], inverse Fourier transform [32], and global optimization algorithms (such as genetic algorithm [33], particle swarm optimization algorithm [34] and neural network [35]) have been successfully applied to reconstruct the corrupted elements.

The remainder of this paper is organized as follows. Section II presents the problem formulation. Section III shows the proposed solution based on ℓ_p -norm. Section IV introduces the application of our algorithm under reverberation and the superiority over other related algorithms. Finally, Section V draws conclusions.

II Problem Formulation

Assume there are r underwater targets from unknown distinct direction of $\{\theta_1, \dots, \theta_r\}$ impinging on the VLA which has N sensors with array spacing of half-wave. Moreover, we use $\mathbf{A}(\theta) \in \mathbb{C}^{N \times r}$ to denote the steering matrix of all the steering vectors. It is also assumed that the DOAs of the source are not time-varying and the number of snapshots is M . Then, we have

$$\mathbf{X} = (\mathbf{A}(\theta)\mathbf{S} + \mathbf{R})^T. \quad (1)$$

In (1), $\mathbf{X} = [\mathbf{x}_1, \mathbf{x}_2, \dots, \mathbf{x}_N] \in \mathbb{C}^{M \times N}$ is the array data matrix, and the n th element \mathbf{x}_n of \mathbf{X} denotes the samples of sensor n . Moreover, $\mathbf{S} = [\mathbf{s}_1, \mathbf{s}_2, \dots, \mathbf{s}_M] \in \mathbb{C}^{r \times M}$ is the signal matrix, where \mathbf{s}_m represents the signal vector at time instant m . $\mathbf{R} \in \mathbb{C}^{N \times M}$ is the measured reverberation matrix. In practical systems, we usually have $r < N < M$. Therefore, $\mathbf{M} = \mathbf{A}(\theta)\mathbf{S} \in \mathbb{C}^{N \times M}$ is a low-rank matrix.

In order to model sensor failure in sonar array, the following two cases illustrated in Fig. 2 will be investigated: (a) Some hydrophones are failed during the entire sampling period, and the missing positions of channel are randomly selected. (b) Some hydrophones are failed during the entire sampling period, and

the missing positions of channel are randomly and continuously selected. When the array is corrupted

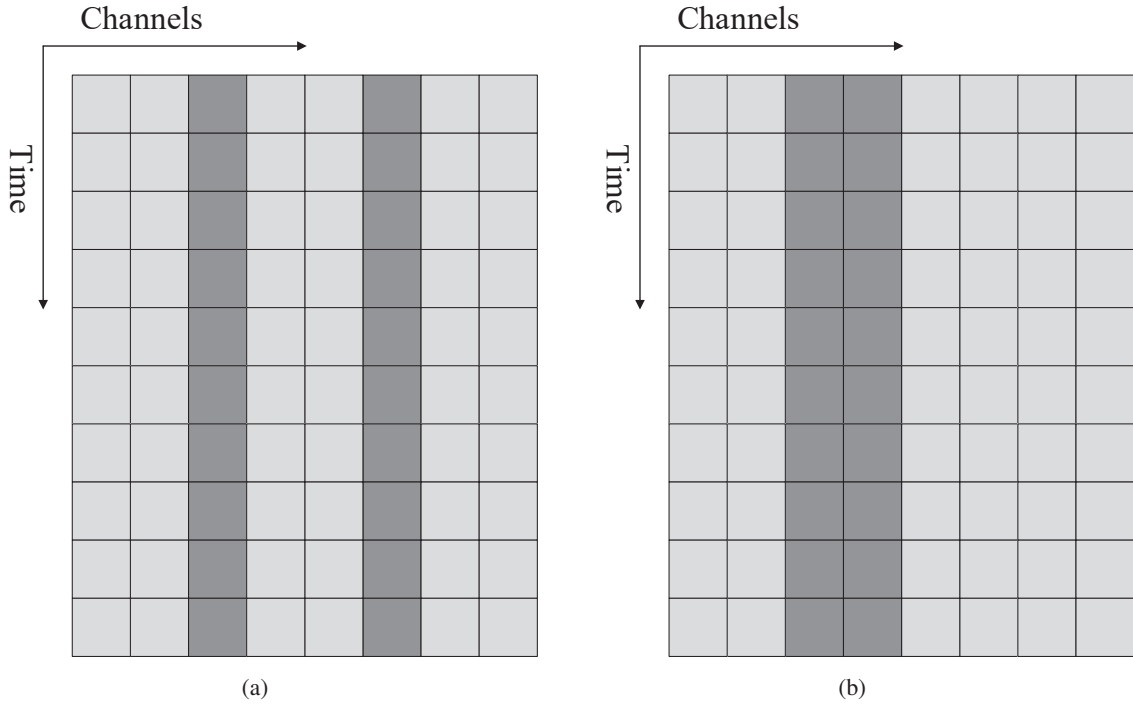


Fig. 2: The model of sensor failure in sonar array.

with sensor failure, the incomplete measurement matrix can be written as

$$\mathbf{X} = \mathbf{B} \odot (\mathbf{M} + \mathbf{R})^T. \quad (2)$$

In (2), \mathbf{B} is a binary matrix composed of 0 and 1 at the positions associated with normal and corrupted data, respectively. \odot denotes element-wise product. In this paper, we assume \mathbf{B} has been judged by the received acoustic data. Moreover, we define the operator \mathcal{P}_Ω as $[\mathcal{P}_\Omega(\mathbf{X})]_{i,j} = X_{i,j}$ if $(i,j) \in \Omega$ and 0 otherwise, where $\Omega \in \{1, \dots, M\} \times \{1, \dots, N\}$ contains the indices of observed entries.

With the improvement of sonar resolution, it leads a fact that the number of effective ocean scatterers in each spatial processing unit is greatly reduced, which no longer meets the central limit theorem in statistics. The envelope of reverberation $\mathbf{R}_e(x)$ of high-resolution sonar has serious smearing. Therefore, it is with skewness and no longer obeys the Gaussian distribution. So, we can regard the ocean reverberation as outliers in the receiver matrix. The statistical properties have been investigated by some experimental data, and in this paper we choose the K distribution to describe the reverberation [44–46] which can be determined by different degrees of freedom n . Moreover, the phase $\mathbf{R}_p(\varphi)$ can be described by the

uniform distribution:

$$\mathbf{R}_e(x) = \begin{cases} \frac{1}{2^{n/2}\Gamma(n/2)}x^{\frac{n}{2}-1}e^{-x/2}, & \text{if } x > 0 \\ 0, & \text{else} \end{cases}, \quad (3)$$

$$\mathbf{R}_p(\varphi) = \begin{cases} \frac{1}{2\pi}, & \text{if } \varphi \in (0, 2\pi) \\ 0, & \text{else} \end{cases}. \quad (4)$$

Accordingly, the reverberation signal \mathbf{R} in (1) can be obtained by

$$\mathbf{R} = \mathbf{R}_e(x)e^{j\mathbf{R}_p(\varphi)}. \quad (5)$$

In the absence and corruption of data, it is known that PCA is a common approach to data analysis and dimensionality reduction, e.g., information extraction such as DOA estimation. However, if the entries in the observation matrix are severely damaged, the error between the matrix obtained by PCA and the original matrix will be very large. This is mainly because PCA is sensitive to outliers. The accurate calculation of principal components in the presence of outliers is called robust principal component analysis (RPCA) [36, 37]. The MC [38] theory proposed by Candès *et al.* is an important method for data analysis and processing after the CS theory. CS and MC are the main components of principal component pursuit (PCP) [39, 40], which can be used to solve RPCA. When the data matrix is severely damaged or corrupted by noise, MC is capable of the near-perfect recovery of matrices if the original matrices have low rank characteristics. Motivated by the advantages of MC techniques, in this paper, we propose to utilize the low-rank matrix factorization to recover the acoustic data caused by sonar sensor failure in ocean reverberation. Note that the conventional techniques for MC depend on the assumption of Gaussian interference; however, in the ocean environment, the background of noise is usually non-Gaussian. Zeng and So [41] have proved that ℓ_p -norm with $0 < p < 2$ shows a better performance than the Frobenius norm in the presence of outliers. Thus, with the reverberation signal in simulation, ℓ_1 -norm and ℓ_2 -norm are utilized to reply to reverberation suppression, and Hankel structured matrix is employed to deal with sensor failure.

From the MC theory we know that when the entries of a certain row or column of a matrix are completely missing, generally, the missing entries cannot be directly recovered based on other entries. One solution is converting the matrix into a Hankel structured matrix, and then applying the MC theory to recover the missing entries. Let $\mathcal{H}_{n_1} : \mathbf{X} \in \mathbb{C}^{M \times N} \rightarrow \mathbf{Z} \in \mathbb{C}^{Mn_1 \times n_2}$ denote a linear operator, mapping

the data matrix into the corresponding Hankel matrix [42]:

$$\mathcal{H}_{n_1}(\mathbf{X}) = \begin{bmatrix} \mathbf{x}_1 & \mathbf{x}_2 & \cdots & \mathbf{x}_{n_2} \\ \mathbf{x}_2 & \mathbf{x}_3 & \cdots & \mathbf{x}_{n_2+1} \\ \vdots & \vdots & \ddots & \vdots \\ \mathbf{x}_{n_1} & \mathbf{x}_{n_1+1} & \cdots & \mathbf{x}_N \end{bmatrix}, \quad (6)$$

where $n_1 + n_2 = N + 1$, and we usually take $n_1 = N/2$. It is not difficult to find that even if some columns of the original data matrix are missing, in the new reshaped Hankel matrix, the coordinates of the missing entries have been all shuffled, so the situation of all missing entries of some columns will no longer occur. In our paper, for simplicity, we use $\mathcal{H}(\mathbf{X})$ instead of $\mathcal{H}_{n_1}(\mathbf{X})$. For example, we assume that an original matrix is

$$\mathbf{X} = \begin{bmatrix} 1 & 4 & 7 & 10 \\ 2 & 5 & 8 & 11 \\ 3 & 6 & 9 & 12 \end{bmatrix}. \quad (7)$$

If column 2 of \mathbf{X} corrupts, the unobserved entries over Ω is $\{(1, 2), (2, 2), (3, 2)\}$. Then, we have

$$\mathcal{P}_\Omega(\mathbf{X}) = \begin{bmatrix} 1 & \times & 7 & 10 \\ 2 & \times & 8 & 11 \\ 3 & \times & 9 & 12 \end{bmatrix}, \quad (8)$$

whose Hankel structured matrix is

$$\mathcal{H}(\mathcal{P}_\Omega(\mathbf{X})) = \begin{bmatrix} 1 & \times & 7 \\ 2 & \times & 8 \\ 3 & \times & 9 \\ \times & 7 & 10 \\ \times & 8 & 11 \\ \times & 9 & 12 \end{bmatrix}. \quad (9)$$

After the Hankel transformation, $\Omega \rightarrow \Omega'$, the unobserved entries over Ω' are $\{(1, 2), (2, 2), (3, 2), (4, 1), (5, 1), (6, 1)\}$. Accordingly, the inverse Hankel transformation of \mathcal{H} , i.e., \mathcal{H}^\dagger , $\mathcal{H}^\dagger(\mathbf{Z}) \in \mathbb{C}^{M \times N}$ [42] is given by

$$(\mathcal{H}^\dagger(\mathbf{Z}))_{i,j} = \frac{1}{w_j} \sum_{k_1+k_2=j+1} Z_{(k_1-1)n_c+i,k_2}, \quad (10)$$

Algorithm 1 : Hankel Structured MC Based on ℓ_p -norm

Input: \mathbf{X}_Ω , Ω , \mathbf{B} , r and the iteration times K .

- 1: **Preprocess** : $\mathbf{X} \rightarrow \mathcal{H}(\mathbf{X})$.
- 2: $\Omega \in \mathbb{C}^{M \times N} \rightarrow \Omega' = \mathcal{H}(\mathbf{B}) \in \mathbb{C}^{Mn_1 \times n_2}$.
- 3: **Initialize** : Randomly initialize $\mathbf{U}^0 \in \mathbb{R}^{Mn_1 \times r}$.
- 4: Determine $\{\mathcal{I}_{jj}\}_{jj=1}^{n_2}$ and $\{\mathcal{J}_{ii}\}_{ii=1}^{Mn_1}$ according to Ω' .
- 5: **for** $k = 0, 1, \dots, K$ **do**
- 6: **for** $jj = 1, 2, \dots, n_2$ **do**
- 7: $(\mathbf{v}_{jj})^{k+1} \leftarrow \arg \min_{\mathbf{v}_{jj}} \|\mathbf{b}_{\mathcal{I}_{jj}} - \mathbf{U}_{\mathcal{I}_{jj}}^k \mathbf{v}_{jj}\|_p^p$.
- 8: **end for**
- 9: **for** $ii = 1, 2, \dots, Mn_1$ **do**
- 10: $(\mathbf{u}_{ii}^T)^{k+1} \leftarrow \arg \min_{\mathbf{u}_{ii}^T} \|\mathbf{b}_{\mathcal{J}_{ii}}^T - \mathbf{u}_{ii}^T \mathbf{V}_{\mathcal{J}_{ii}}^{k+1}\|_p^p$.
- 11: **end for**
- 12: **end for**

Output: $\mathbf{M} = \mathcal{H}^\dagger(\mathbf{U}^{k+1} \mathbf{V}^{k+1})$.

where w_j is the number of elements in the j th anti-diagonal. For example, the 3rd anti-diagonal contains three elements over $\{(3, 1), (2, 2), (1, 3)\}$, so $w_3 = 3$; and the N th anti-diagonal contains only one elements, so $w_N = 1$.

The task of MC in this paper aims at recovering \mathbf{M} from $\mathcal{P}_\Omega(\mathbf{X})$, and the corresponding optimization problem is formulated as

$$\begin{aligned} \min_{\mathbf{M}, \mathbf{R}} \quad & \|\mathcal{H}(\mathcal{P}_\Omega(\mathbf{X})) - \mathcal{H}(\mathcal{P}_\Omega(\mathbf{M}^T))\|_p^p, \\ \text{s.t.} \quad & \text{rank}(\mathcal{H}(\mathbf{M}^T)) \leq r \end{aligned} \quad (11)$$

where $\|\cdot\|_p$ is the l_p norm of a matrix, i.e.,

$$\|\mathbf{E}_\Omega\|_p = \left(\sum_{(i,j) \in \Omega} \|\mathbf{E}_{i,j}\|^p \right)^{1/p}. \quad (12)$$

In (12), $\mathbf{E}_\Omega = \mathcal{H}(\mathcal{P}_\Omega(\mathbf{X})) - \mathcal{H}(\mathcal{P}_\Omega(\mathbf{M}^T))$ denotes the error matrix. It is worth mentioning that we consider two situations $p = 1$ and $p = 2$ in this paper. As the solution procedure is executed based on the Hankel structure, problem (11) is equivalent to

$$\begin{aligned} \min_{\mathbf{M}, \mathbf{R}} \quad & \|(\mathcal{H}(\mathbf{X}))_{\Omega'} - (\mathcal{H}(\mathbf{M}^T))_{\Omega'}\|_p^p, \\ \text{s.t.} \quad & \text{rank}(\mathcal{H}(\mathbf{M}^T)) \leq r \end{aligned} \quad (13)$$

The minimization with the observed entries is made a transitions from Ω to Ω' .

III Hankel structured MC based ℓ_p -norm

Low rank matrix factorization [41], which is considered as the low rank property of matrix, has been used to void full singular value decomposition (SVD). Therefore, optimization problem (13) can be transformed into

$$\min_{\mathbf{U}, \mathbf{V}} f_p(\mathbf{U}, \mathbf{V}) := \| (\mathcal{H}(\mathbf{X}))_{\Omega'} - (\mathbf{UV})_{\Omega'} \|_p^p, \quad (14)$$

where $\mathbf{U} \in \mathbb{C}^{Mn_1 \times r}$ and $\mathbf{V} \in \mathbb{C}^{r \times n_2}$. Because $r \ll Mn_1n_2$, the complexity of MC will be greatly reduced. Furthermore, the smaller the rank r , the higher the accuracy of MC. The error matrix after Hankel structured processing can be rewritten as $\mathbf{E}_{\Omega'} = (\mathcal{H}(\mathbf{X}))_{\Omega'} - (\mathbf{UV})_{\Omega'}$. It is worth noting that the inverse Hankel transformation in (10) needs to be operated with $\widehat{\mathbf{M}} = (\mathcal{H}^\dagger(\mathbf{UV}))^T$ when \mathbf{U} and \mathbf{V} have been determined.

The strategy of alternating minimization with a relaxation as a bi-convex problem is adopted to solve \mathbf{U} and \mathbf{V} respectively according to:

$$\mathbf{V}^{k+1} = \arg \min_{\mathbf{V}} \| (\mathcal{H}(\mathbf{X}))_{\Omega'} - (\mathbf{U}^k \mathbf{V})_{\Omega'} \|_p^p, \quad (15)$$

$$\mathbf{U}^{k+1} = \arg \min_{\mathbf{U}} \| (\mathcal{H}(\mathbf{X}))_{\Omega'} - (\mathbf{UV}^{k+1})_{\Omega'} \|_p^p. \quad (16)$$

In the first step, we solve \mathbf{V} by fixing \mathbf{U} , i.e.,

$$\min_{\mathbf{V}} f_p(\mathbf{V}) := \| (\mathcal{H}(\mathbf{X}))_{\Omega'} - (\mathbf{UV})_{\Omega'} \|_p^p, \quad (17)$$

where $(\cdot)^k$ is omitted for simplicity. Let $\mathbf{u}_{ii}^T \in \mathbb{C}^r$ and $\mathbf{v}_{jj} \in \mathbb{C}^r$ denote the ii th row of \mathbf{U} and the jj th column of \mathbf{V} , respectively, where $ii = 1, \dots, Mn_1$ and $jj = 1, \dots, n_2$. Then, problem (17) can be expressed as follow:

$$\min_{\mathbf{V}} f_p(\mathbf{V}) := \sum_{(ii, jj) \in \Omega'} |(\mathcal{H}(\mathbf{X}))_{ii, jj} - \mathbf{u}_{ii}^T \mathbf{v}_{jj}|^p. \quad (18)$$

According to the number of columns in \mathbf{V} , problem (18) can be decomposed into n_2 independent subproblems:

$$\min_{\mathbf{v}_{jj}} f_p(\mathbf{v}_{jj}) := \sum_{ii \in \mathcal{I}_{jj}} |(\mathcal{H}(\mathbf{X}))_{ii, jj} - \mathbf{u}_{ii}^T \mathbf{v}_{jj}|^p. \quad (19)$$

Here we use $\mathcal{I}_{jj} = \{jj_1, \dots, jj_{|\mathcal{I}_{jj}|}\}$ and $|\mathcal{I}_{jj}|$ to denote the jj th column of Ω' and its cardinality, respectively,

where $|\mathcal{I}_{jj}| > r$. From the Hankel structured matrix given in (9), we know that only the (1, 1), (2, 1) and (3, 1) can be observed when $jj = 1$, so we have $\mathcal{I}_1 = \{1, 2, 3\}$ and $\mathcal{I}_2 = \{4, 5, 6\}$.

Furthermore, we respectively define a matrix $\mathbf{U}_{\mathcal{I}_{jj}} \in \mathbb{C}^{\mathcal{I}_{jj} \times r}$ that contains the observed row indexed by \mathcal{I}_{jj} :

$$\mathbf{U}_{\mathcal{I}_{jj}} = \begin{bmatrix} \mathbf{u}_{jj_1}^T \\ \vdots \\ \mathbf{u}_{jj_{|\mathcal{I}_{jj}|}}^T \end{bmatrix}, \quad (20)$$

and a vector $\mathbf{b}_{\mathcal{I}_{jj}} = [\mathbf{X}_{jj_1, jj}, \dots, \mathbf{X}_{jj_{|\mathcal{I}_{jj}|}, jj}]^T \in \mathbb{C}^{\mathcal{I}_{jj}}$. Then, problem (19) is equivalent to

$$\min_{\mathbf{v}_{jj}} f_p(\mathbf{v}_{jj}) := \|\mathbf{b}_{\mathcal{I}_{jj}} - \mathbf{U}_{\mathcal{I}_{jj}} \mathbf{v}_{jj}\|_p^p. \quad (21)$$

When $p = 2$, problem (21) becomes a least squares problem and can be solved by $\mathbf{v}_{jj} = \mathbf{U}_{\mathcal{I}_{jj}}^\dagger \mathbf{b}_{\mathcal{I}_{jj}}$, and the implementary complexity of the jj th iteration is $\mathcal{O}(|\mathcal{I}_{jj}|r^2)$. When $p = 1$, problem (21) can be solved by the iteratively reweighted least squares (IRLS) algorithm [43]. We use N_{IRLS} to definite the number of iteration of IRLS, and the complexity of jj -iteration here is $\mathcal{O}(|\mathcal{I}_{jj}|r^2 N_{\text{IRLS}})$; moreover, for the n_2 independent subproblems, we have $\sum_{jj=1}^{n_2} |\mathcal{I}_{jj}| = |\Omega'|$, so the overall complexity is $\mathcal{O}(|\Omega'|r^2 N_{\text{IRLS}})$.

As the acoustic data is complex-valued, the real-valued transforms need to be preprocessed in the above algorithm. Then, the real-valued vector of complex-valued $\mathbf{b}_{\mathcal{I}_{jj}} \in \mathbb{C}^{\mathcal{I}_{jj}}$ is

$$\mathbf{b}_{\mathcal{I}_{jj}_r} = \begin{bmatrix} \Re\{\mathbf{b}_{\mathcal{I}_{jj}}\} \\ \Im\{\mathbf{b}_{\mathcal{I}_{jj}}\} \end{bmatrix} \in \mathbb{R}^{2\mathcal{I}_{jj}}. \quad (22)$$

Besides, the real-valued matrix of complex-valued $\mathbf{U}_{\mathcal{I}_{jj}} \in \mathbb{C}^{\mathcal{I}_{jj} \times r}$ is

$$\mathbf{U}_{\mathcal{I}_{jj}_r} = \begin{bmatrix} \Re\{\mathbf{U}_{\mathcal{I}_{jj}}\} & -\Im\{\mathbf{U}_{\mathcal{I}_{jj}}\} \\ \Im\{\mathbf{U}_{\mathcal{I}_{jj}}\} & \Re\{\mathbf{U}_{\mathcal{I}_{jj}}\} \end{bmatrix} \in \mathbb{R}^{(2\mathcal{I}_{jj}) \times (2r)}. \quad (23)$$

Similarly, the ii th row of \mathbf{U} can be also solved trough Mn_1 independent subproblems:

$$\min_{\mathbf{u}_{ii}^T} f_p(\mathbf{u}_{ii}^T) := \|\mathbf{b}_{\mathcal{J}_{ii}}^T - \mathbf{u}_{ii}^T \mathbf{V}_{\mathcal{J}_{ii}}\|_p^p, \quad (24)$$

where $\mathbf{V}_{\mathcal{J}_{ii}} \in \mathbb{C}^{r \times \mathcal{J}_{ii}}$ and $\mathbf{b}_{\mathcal{J}_{ii}}^T = [\mathbf{X}_{ii, ii_1}, \dots, \mathbf{X}_{ii, ii_{\mathcal{J}_{ii}}}]^T \in \mathbb{C}^{\mathcal{J}_{ii}}$, and $\mathcal{J}_{ii} = \{ii_1, \dots, ii_{\mathcal{J}_{ii}}\} \in \{1, \dots, n_2\}$ denotes the column for the ii th row in Ω' . In (9), when $ii = 1$, we have $\mathcal{J}_1 = \mathcal{J}_2 = \mathcal{J}_3 = \{1, 3\}$ and $\mathcal{J}_4 = \mathcal{J}_5 = \mathcal{J}_6 = \{2, 3\}$.

Above all, the proposed algorithm consists of two stages. The first stage preprocesses \mathbf{X} into $\mathcal{H}(\mathbf{X})$, and then converts Ω into Ω' . The second stage fulfills the MC with ℓ_p -norm in Ω' . The overall complexity of the proposed algorithm is $\mathcal{O}(|\Omega'|r^2N_{\text{IRLS}}K)$, where K is the iteration times.

IV Applications in reverberation suppression

In this paper, we use the SRR defined as follow to compare the level of the target signal with the reverberation:

$$\text{SSR} = 10 \log_{10} \left(\frac{\sigma_s^2}{\sigma_n^2} \right) \text{ dB}, \quad (25)$$

where σ_s^2 and σ_n^2 are the variances of signal and reverberation, respectively.

Moreover, the normalized root mean square error (RMSE) defined as follows is exploited to measure the performance based on 100 independent trials:

$$\text{RMSE}(\widehat{\mathbf{M}}) = \sqrt{\text{E} \left\{ \frac{\|\widehat{\mathbf{M}} - \mathbf{M}\|_F^2}{\|\mathbf{M}\|_F^2} \right\}}, \quad (26)$$

where $\widehat{\mathbf{M}}$ is the result obtained by equations (12) and (13). A typical experimental setting is $N = 20$, $M = 100$, and $r = 2$. We compare the proposed algorithm respectively based on ℓ_1 -norm and ℓ_2 -norm with OptSpace [47] and structured alternating projection (SAP) [42] to recover \mathbf{M} from $\mathcal{P}_\Omega(\mathbf{X})$.

Fig. 3 plots the normalized RMSE versus the iteration times. We set $\text{SSR} = 10$, and the sensor failure percentage is 30%, and the degrees of freedom of K distribution is $n = 0.1$. We can observe that the OptSpace algorithm exhibits a high error without falling. Moreover, the SAP and ℓ_2 -norm begin to converge and they have almost same the RMSEs. Besides, they also provide robust performances in the ocean reverberation. However, their performances are still worse than that of of the ℓ_1 -norm. Finally, it can be observed that the algorithms of SAP, ℓ_1 - and ℓ_2 -norms converge within ten iterations.

Fig. 4 illustrates the SSR with respect to the probability of recovery. For each realization, 100 independent trials were evaluated. Firstly, if the normalized RMSE is smaller than 0.15, we think that the trial is successful and observed as white region, and dark region otherwise. Moreover, we can observe that the algorithm based on ℓ_1 -norm has the best performance than others in the ocean reverberation. Besides, the algorithm of OptSpace is only valid when the SSR is above 10 dB and the sensor failure percentage

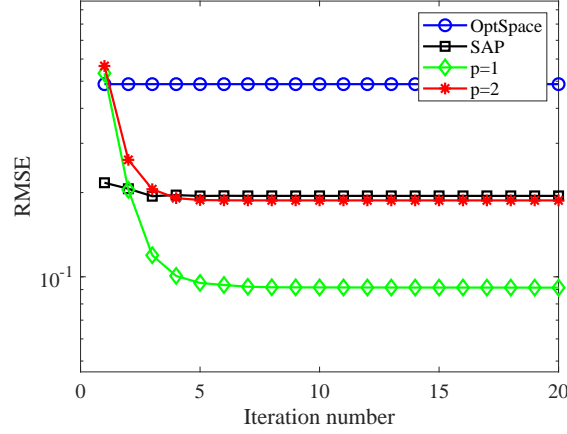


Fig. 3: The normalized RMSE versus iteration number.

is smaller than 10%. It is also worth noting that the SAP and algorithm based on ℓ_2 -norm have similar performances. Therefore, the MC algorithm based on ℓ_1 -norm is suitable for the reverberation suppression.

In this paper, the performance of DOA estimation is measured in terms of the RMSE:

$$\text{RMSE}(\hat{\theta}) = \sqrt{\frac{1}{100r} \sum_{p=1}^r \sum_{q=1}^{100} (\hat{\theta}_{q,p} - \theta_q)^2}, \quad (27)$$

where $\hat{\theta}$ is the estimated DOA.

Fig. 5 shows the normalized spectrum versus bearing angle in degrees. Due to the effect of sensor failure and reverberation interference on the original data, the normalized spectrum appears false peaks. Hence, the beam pattern is sensitive to the contaminated signal. Besides, the main lobe of the OptSpace algorithm converges to the true signal orientation, but there are certain apparent estimation errors. Thirdly, the algorithms of SAP and ℓ_2 -norm have obvious performance improvements, and both of them can make more accurate spectrum estimation and have almost the same performances. Fourthly, the algorithm based on ℓ_1 -norm exhibits the narrowest beamwidth and lowest sidelobe compared with other algorithms. Most importantly, the algorithm based on ℓ_1 -norm has the best robustness of spectrum estimation in the ocean reverberation with sensor failure.

According to Fig. 4, we choose the sensor failure percentage less than 50% for the comparison of DOA estimation because of the high probability of recovery. Fig. 6 shows the results of RMSE versus SSR and sensor failure percentage, where the threshold of normalized RMSE of DOA is chosen as 0.15. Firstly, if the RMSE is smaller than 0.15, the result can be observed as white region and dark region otherwise. Furthermore, the original data with sensor failure and reverberation interference cause large errors along

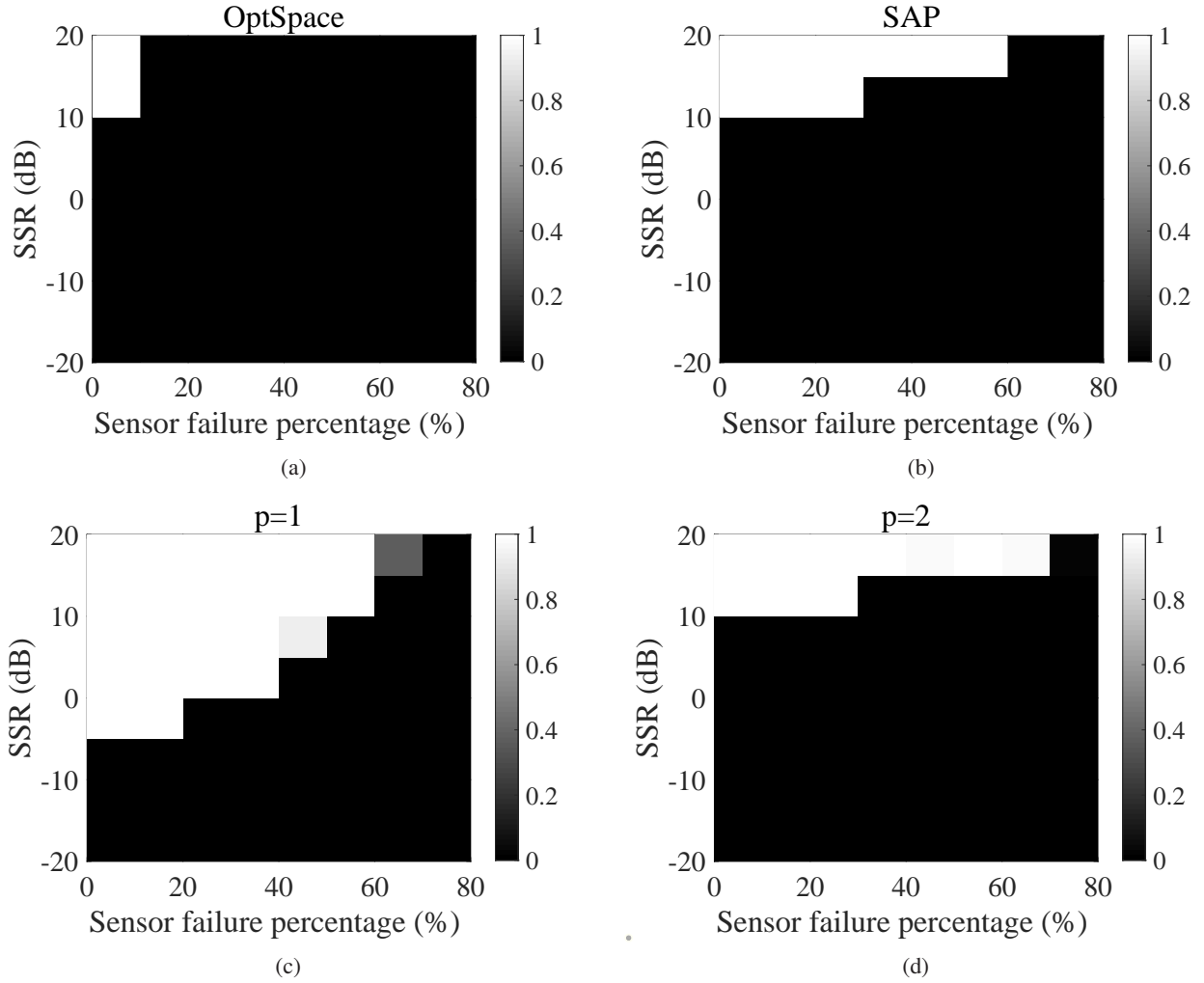


Fig. 4: The probability of recovery versus SSR and sensor failure percentage.

with different SSRs, in which the all normalized RMSEs definitely exceed 0.15 and show a whole dark region in Fig. 6 (a). From Fig. 6 (b)~(e) it can also be observed that the MC algorithms of OptSpace, SAP and ℓ_p -norm with the receiving acoustic data have a constructive influence on the DOA estimation. Thirdly, when the SSR is above 5 dB, there are all almost no errors of DOA with the involved algorithms. As for the SSR less than 5 dB, the errors of DOA achieved by the algorithm with ℓ_1 -norm will be less. Accordingly, the MC algorithm with ℓ_1 -norm is suitable for source location in the ocean reverberation environment with sensor failure, especially for low SSR.

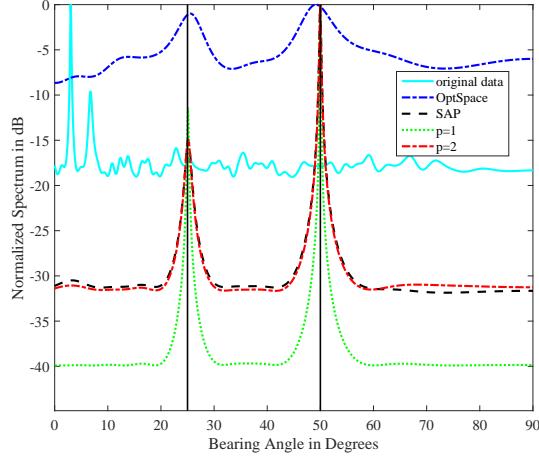


Fig. 5: The comparison of beam pattern.

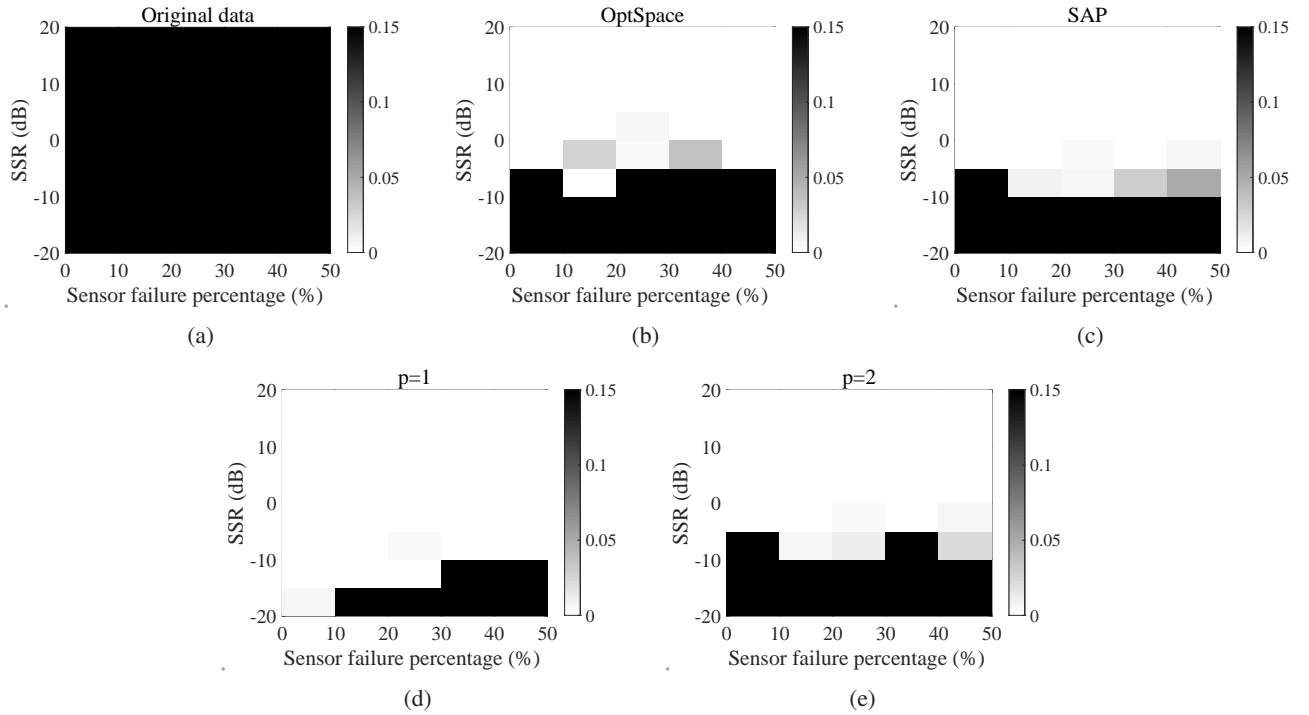


Fig. 6: RMSE (θ) versus SSR and sensor failure percentage.

V Conclusion

This paper proposed an approach of acoustic localization in the presence of ocean reverberation with sonar sensor failure. First, the model of sensor failure is established, and the Hankel structured matrix is transformed for the received incomplete matrix. Then, the ocean reverberation is regarded as outliers in the received matrix. With the low rank factorization, the algorithms of ℓ_1 - and ℓ_2 - norms are developed

to recover the signal matrix in the ocean, which can converge to the ground-truth matrix ultimately. The algorithm based on ℓ_1 -norm is suitable for reverberation suppression because of the narrow beam width and low sidelobe. The results show that the robustness of acoustic localization in the ocean reverberation with sensor failure can be improved by the matrix completion with ℓ_1 -norm minimization.

*Bibliography

- [1] K. Yang, L. Xu, Q. Yang, and G. Li, "Two-step inversion of geoacoustic parameters with bottom reverberation and transmission loss in the deep ocean," *Acoustics Australia*, vol. 46, no. 1, pp. 131–142, 2018.
- [2] P. C. Etter, *Underwater acoustic modeling and simulation, Fourth Edition*. CRC, New York, 2013.
- [3] Y. Doisy, L. Deruaz-Pepin, and P. Beerens, "Sonar waveforms for reverberation rejection, part i: theory," in *Proc. UDT Pacific*. TNO Fysisch en Elektronisch Laboratorium, 2000.
- [4] Y. Doisy, L. Deruaz-Pepin, and P. Beerens, "Sonar waveforms for reverberation rejection, part ii: experimental results," in *Proc. UDT Pacific*. TNO Fysisch en Elektronisch Laboratorium, 2000.
- [5] J. Maksym and M. Sandys-Wunsch, "Adaptive beamforming against reverberation for a three-sensor array," *J. Acoust. Soc. Am.*, vol. 102, no. 6, pp. 3433–3438, 1997.
- [6] I. Schurman, "Reverberation rejection with a dual-line towed array," *IEEE J. Oceanic Eng.*, vol. 21, no. 2, pp. 193–204, 1996.
- [7] D. Gingras, "Single mode excitation, attenuation, and backscatter in shallow water," *J. Acoust. Soc. Am.*, vol. 103, no. 1, pp. 195–204, 1998.
- [8] J. Arvelo and X. Zabal, "Reverberation rejection via modeforming with a vertical line array," *IEEE J. Oceanic Eng.*, vol. 22, no. 3, pp. 541–547, 1997.
- [9] A. Gershman, U. Nickel, and J. Böhme, "Adaptive beamforming algorithms with robustness against jammer motion," *IEEE Trans. Signal Process*, vol. 45, no. 7, pp. 1878–1885, 1997.
- [10] D. Tufts, H. Ge, and S. Umesh, "Fast maximum likelihood estimation of signal parameters using the shape of the compressed likelihood function," *IEEE J. Oceanic Eng.*, vol. 18, no. 4, pp. 388–400, 1993.
- [11] Y. Ge, T. Yang, and S. Piao, "Estimating the delay-doppler of target echo in a high clutter underwater environment using wideband linear chirp signals: Evaluation of performance with experimental data," *J. Acoust. Soc. Am.*, vol. 124, no. 4, pp. 2047–2057, 2017.
- [12] S. Kim, W. Kuperman, W. Hodgkiss, and H. Song, "Echo-to-reverberation enhancement using a time

- reversal mirror,” *J. Acoust. Soc. Am.*, vol. 115, no. 4, pp. 1125–1131, 2004.
- [13] H. Song, S. Kim, W. Hodgkiss, and W. Kuperman, “Environmentally adaptive reverberation nulling using a time reversal mirror,” *J. Acoust. Soc. Am.*, vol. 116, no. 2, pp. 762–768, 2004.
- [14] H. Song, W. Hodgkiss, W. Kuperman, P. Roux, T. Akal, and M. Stevenson, “Experimental demonstration of adaptive reverberation nulling using a time reversal,” *J. Acoust. Soc. Am.*, vol. 118, no. 3, pp. 1381–1387, 2005.
- [15] D. Malioutov, M. cetin, and A. Willsky, “A sparse signal reconstruction perspective for source localization with sensor arrays,” *IEEE Trans. Signal Process*, vol. 53, no. 8, pp. 3010–3022, 2005.
- [16] P. Gerstoft, C. F. Mecklenbräuker, W. Seong, and M. Bianco, “Introduction to compressive sensing in acoustic,” *J. Acoust. Soc. Am.*, vol. 143, no. 6, pp. 3731–3736, 2018.
- [17] Y. Choo, Y. Park, and W. Seong, “Compressive time-domain beamforming,” in *Proc. IEEE Underwater Technology*, 2017.
- [18] J. Zheng and M. Kaveh, “Sparse spatial spectral estimation: A covariance fitting algorithm, performance and regularization,” *IEEE Trans. Signal Process*, vol. 61, no. 11, pp. 2767–2777, 2013.
- [19] Y. Ge, S. Piao, and X. Han, “Fractional fourier transform-based detection and delay time estimation of moving target in strong reverberation environment,” *IET Radar, Sonar and Nav.*, vol. 11, no. 9, pp. 1367–1372, 2017.
- [20] Y. Zhu, K. Yang, R. Duan, and F. Wu, “Fractional fourier transform-based detection and delay time estimation of moving target in strong reverberation environment,” *Appl. Acoust.*, vol. 160, p. 107132, 2020.
- [21] G. Ginolhac and G. Jourdain, “Principal component inverse algorithm for detection in the presence of reverberation,” *IEEE J. Oceanic Eng.*, vol. 27, no. 2, pp. 310–321, 2002.
- [22] L. Kirsteins and D. Tufts, “Adaptive detection using low rank approximation to a data matrix,” *IEEE Trans. Aero. Elec. Sys.*, vol. 30, no. 1, pp. 55–67, 1994.
- [23] T. J. Peters, “A conjugate gradient-based algorithm to minimize the sidelobe level of planar arrays with element failures,” *IEEE Trans. Antenn. Propag.*, vol. 39, no. 10, pp. 1497–1504, 1991.
- [24] M. Er and S. Hui, “Beamforming in presence of element failure,” *IEEE Electron. Lett.*, vol. 27, no. 3, pp. 273–275, 1991.
- [25] M. Lozano, J. A. R. Gonzalez, and F. Ares, “Recalculating linear array antennas to compensate for failed elements while maintaining fixed nulls,” *J. Electromagnet. Wave.*, vol. 13, no. 3, pp. 2048–

2051, 1999.

- [26] S. Sim and M. Er, "Sidelobe suppression for general arrays in presence of element failures," *IEEE Electron. Lett.*, vol. 33, no. 15, pp. 1278–1280, 1997.
- [27] S. H. Zainud-Deen, M. Ibrahim, H. Sharshar, and S. Ibrahim, "Array failure correction with orthogonal methods," in *Proc. 21th National Radio Science Conference*, 2004.
- [28] R. J. Mailloux, "Array failure correction with a digitally beamformed array," *IEEE Trans. Antenn. Propag.*, vol. 44, no. 12, pp. 1543–1550, 1996.
- [29] H. Steyskal and R. J. Mailloux, "Generalisation of an array-failure-correction method," in *Proc. Microw. Antennas and Propag.*, vol. 145, no. 4, 1998, pp. 332–336.
- [30] S. Bu and A. Daryoush, "Comparison of reconfigurable methods of active phased array antenna," in *Proc. Antennas and Propagation Society International Symposium*, Aug, 1993, pp. 214–217.
- [31] M. Dogan and J. M. Mendel, "Applications of cumulants to array processing-part i. aperture extension and array calibration," *IEEE Trans. Signal Process.*, vol. 43, no. 5, pp. 1200–1216, 1995.
- [32] W. P. N. Keizer, "Element failure correction for a large monopulse phased array antenna with active amplitude weighting," *IEEE Trans. Antenn. Propag.*, vol. 55, no. 8, pp. 2211–2218, 2007.
- [33] J. H. Han, S. H. Lim, and N. H. Myung, "Array antenna trm failure compensation using adaptively weighted beam pattern mask based on genetic algorithm," *IEEE Antenn. Wirel. Pr.*, vol. 11, pp. 18–21, 2012.
- [34] D. W. Boeringer and D. H. Werner, "Particle swarm optimization versus genetic algorithms for phased array synthesis," *IEEE Trans. Antenn. Propag.*, vol. 52, no. 3, pp. 771–779, 2004.
- [35] S. Vigneshwaran, N. Sundararajan, and P. Saratchandran, "Direction of arrival (doa) estimation under array sensor failures using a minimal resource allocation neural network," *IEEE Trans. Antenn. Propag.*, vol. 55, no. 2, pp. 334–343, 2007.
- [36] H. Xu, C. Caramanis, and S. Sanghavi, "Robust pca via outlier pursuit," *IEEE Trans. Inform. Theory*, vol. 58, no. 5, pp. 3047–3064, 2012.
- [37] C. Qiu, N. Vaswani, B. Lois, and L. Hogben, "Recursive robust pca or recursive sparse recovery in large but structured noise," *IEEE Trans. Inform. Theory*, vol. 60, no. 8, pp. 5007–5039, 2013.
- [38] E. Candes and Y. Plan, "Matrix completion with noise," in *Proc. of the IEEE*, vol. 98, no. 6, 2010, pp. 925–936.
- [39] E. J. Candes, X. Li, Y. Ma, and J. Wright, "Robust principal component analysis?" *J. ACM*, vol. 58,

no. 3, pp. 1–39, 2009.

- [40] G. Han, C. Qiu, and N. Vaswani, “An online algorithm for separating sparse and low-dimensional signal sequences from their sum,” *IEEE Trans. Signal Process.*, vol. 62, no. 16, pp. 4284–4297, 2014.
- [41] W. Zeng and H. C. So, “Outlier-robust matrix completion via ℓ_p -minimization,” *IEEE Trans. Signal Process.*, vol. 66, no. 5, pp. 1125–1140, 2018.
- [42] S. Zhang and M. Wang, “Correction of corrupted columns through fast robust hankel matrix completion,” *IEEE Trans. Signal Process.*, vol. 67, no. 10, pp. 2580–2594, 2019.
- [43] D. P. Leary, “Robust regression computation using iteratively reweighted least squares,” *SIAM. J. Matrix Anal. Appl.*, vol. 11, no. 3, pp. 466–480, 1990.
- [44] D. Middleton, “New physical-statistical methods and models for clutter and reverberation: the ka-distribution and related probability structures,” *IEEE J. Ocean. Eng.*, vol. 24, no. 3, pp. 261–284, 1999.
- [45] D. A. Abraham and A. P. Lyons, “Novel physical interpretations of kdistributed reverberation,” *IEEE J. Ocean. Eng.*, vol. 27, no. 4, pp. 800–813, 2002.
- [46] D. P. Leary, “Exponential scattering and kdistributed reverberation,” *D.A. Abraham and A.P.Lyons*, vol. 3, pp. 1622–1628, 2001.
- [47] R. H. Keshavan and S. Oh, “A gradient descent algorithm on the grassman manifold for matrix completion,” *arXiv: 0910 5260v2*, pp. 1–26, 2009.